OPEN ACCESS

University of Dundee

University of Dundee

Periprostatic Fat Adipokines Expression Correlated with Prostate Cancer Aggressiveness in Men Undergoing Radical Prostatectomy for Clinically Localised Disease

Dahran, Naief; Szewczyk-Bieda, Magdalena; Vinnicombe, Sarah; Fleming, Stewart; Nabi, Ghulam

Periprostatic Fat Adipokines Expression Correlated with Prostate Cancer Aggressiveness in Men Undergoing Radical Prostatectomy for Clinically Localised Disease

Naief Dahran[a,b], Magdalena Szewczyk-Bieda[a], Sarah Vinnicombe[a], Stewart Fleming[a], *Ghulam Nabi[a]

[a] Division of Cancer Research, School of Medicine, University of Dundee, Dundee, DD1 9SY, UK.
[b] Department of Anatomy, Faculty of Medicine, University of Jeddah, Jeddah, Saudi Arabia.

*Correspondence to:
Professor Ghulam Nabi
Professor of Surgical Uro-Oncology & Consultant Urological Surgeon,
Head of Division for Cancer Research,
Division of Cancer Research, School of Medicine,
University of Dundee
Email: g.nabi@dundee.ac.uk

Abstract

Objectives: To investigate relationship between periprostatic adipose tissue (PPAT) adipokines expression and PCa aggressiveness using both pathological features of radical prostatectomy (RP) and multiparametric MRI parameters.

Patients and methods: Sixty-nine men were recruited to assess immunohistochemical expression of TNFα- and VEGF of periprostatic fat of radical prostate specimens. Percent immunopositivity was quantified on scanned slides using Aperio Positive Pixel Count algorithm for PPAT TNFα, VEGF and androgen receptors. Periprostatic fat volume (PFV) was segmented on contiguous T_1-weighted axial MRI slices from the level of the prostate base to apex. PFV was normalised to prostate volume (PV) to account for variations in PV (NPFV=PFV/PV). MRI quantitative values (K_{ep}, K_{trans}, and ADC) were measured from PCa primary lesion using OleaSphere software. Patients were stratified into three groups according to RP GS: ≤6, 7(3+4) and 7(4+3) or more.

Results: The mean rank of VEGF and TNFα were significantly different between the groups [H(2)= 11.038, *p*=0.004] and [H(2)=13.086, *p*=0.001], respectively. Patients with stage pT_3 had higher TNFα (18.2±8.95) positivity than patients with stage pT_2 (13.27±10.66), *t* (67) =-2.03, *p*=0.047. TNFα expression significantly correlated with K_{trans} (ρ=0.327, *p*=0.023). TNFα (*p*=0.043) and VEGF (*p*= 0.02) correlates with high-grade PCa (GS≥7) in radical prostatectomy specimens and correlated significantly with upgradation of Gleason score from biopsy to radical prostatectomy histology.

Conclusions: Expression level of TNFα and VEGF on immunostaining significantly correlated with aggressivity of PCa. As biomarkers, these suggest the risk of having high-grade PCa in men undergoing RP.

1 Introduction

Several studies have found an association between periprostatic fat adiposity and the aggressivity of prostate cancer (PCa) using several different imaging modalities and measurement techniques [1-3]. In a recent MRI study, we found normalised periprostatic fat volume (NPFV) to be a significant predictor for high-grade localised prostate cancer in men opting for radical prostatectomy [4]. However, imaging alone cannot discriminate between metabolically more active and less active periprostatic adipose tissue (PPAT).

Adipocytes have an important role in synthesizing and storing triglycerides from free fatty acids (FFA) and in producing adipokines [5-8]) have reported that there are two kinds of adipocytes: "fat" and "thin". Besides being storage cells for free-fatty acids (the major source of energy for the cancer cell), the more active "fat" cells, which are common in obese populations, may differentiate into "cancer-associated adipocytes" and crosstalk with cancer cells via a paracrine effect, resulting in the secretion of more inflammatory adipokines and chemokines (e.g. CCL7), stimulating macrophage infiltration, which in turn encourages insulin resistance that leads to disease progression and local dissemination [5, 8-13].

Periprostatic adipose tissue inflammation has been found to be associated with high-grade PCa [14]. When adipose tissue expands, hypoxia occurs, and certain adipokines become up-regulated. In response, hypoxia inducible factor 1 alpha (HIF-1α), may interact with endothelial cells and lead to a reduction in nitric oxide that regulates vasodilation, stimulates angiogenesis and increases vascular permeability to overcome the hypoxia [15-17]. Tumour necrosis factor alpha (TNFα) and vascular endothelial growth factor (VEGF) are adipokines which have been widely implicated for their roles in

tumourigenesis by inducing inflammatory and angiogenic responses, respectively, and increasing the risk of metastasis [18-24].

Angiogenesis in periprostatic fat may facilitate the seeding of a PCa microenvironment with adipocyte precursors (lipoblasts), that secrete numerous factors (e.g. IL-6 and TNFα) involved in the inflammatory response, particularly in pathological conditions such as obesity [25]. Zhang et al [26] have described that the tumour microenvironment may contain lipoblasts seeded by visceral fat (VF) through blood vessels. It was suggested that periprostatic fat has more lipoblasts than VF [27]. Thus, periprostatic fat could be a major source for seeding the microenvironment of PCa with lipoblasts, facilitating tumour progression. Understanding the metabolic pathways between PPAT, as an inflammatory promotor, and PCa could reveal new diagnostic and therapeutic possibilities. Anti-angiogenic treatments, in combination with radiotherapy, could be successful ways to treat PCa [28].

This study aimed to:

1. Investigate the correlation between PPAT metabolic activity and prostate cancer aggressiveness by comparing inflammatory and angiogenic adipokine (TNFα and VEGF) expression levels in the periprostatic fat with Gleason scores (GS) and pathological tumour staging (pT).

2. Correlate expression level of adipokines (TNFα and VEGF) with quantifiable MRI parameters of PCa aggressivity.

2 Patients, materials and methods

2.1 Cohort selection and power calculation

This was a prospective study with institutional approval (Caldicott/CSAppGN021211) for follow-up. A sample size of 69 was calculated based on information from a pilot phase of the study ($n = 15$) and a power calculation (**Table S1**). The pilot phase also evaluated the quality of immunostaining. Between January 2010 and December 2015, we recruited 69 men with localised prostate cancer opting for RP. Demographic details were recorded in a database. Periprostatic-fat tissue sections were selected from the excised prostate surface at three or more different periprostatic regions. Tissue block sectioning and immunohistochemistry (IHC) were performed at the Tayside Tissue Biorepository (TBR), Study inclusion criteria were:

- Men with localised prostate cancer (PCa) who underwent Radical Prostatectomy (RP).
- Gleason score and histopathological stage of RP specimens reported and discussed at multidisciplinary meetings by an experienced uropathologist.

Exclusion criteria were: men with metastatic PCa or those with localised disease who had external beam radiotherapy/brachytherapy or focal treatment prior to radical surgery. Men were also excluded if they had hormones in neoadjuvant settings.

The primary aim of the study was evaluation of the magnitude of correlation between the immunohistochemical expression of PPAT and histopathological parameters of PCa. The correlation between quantitative MRI parameters and adipokine expression levels was the secondary aim (**Figure S1**).

2.2   Antibody selection and immunohistochemistry preparation

Table S2 summarises the characteristics of the selected antibodies. Antigen retrieval and deparaffinisation were performed using a DAKO EnVision™ FLEX Target Retrieval solution (high pH) buffer (50x conc.) (K8004) in a DAKO PT Link (serial number PT2794Y1205) for 10 minutes at 97°C. Immunostaining using the DAKO EnVision™ FLEX system on a DAKO Autostainer Link 48 (serial number AS2383D1203) was conducted according to the manufacturer's protocol. Sections were initially washed in a Flex Wash Buffer (K8006). **Table S3** summarises the protocols used for TNFα, VEGF, and AR.

2.3   Immunohistochemistry Analysis

After IHC application, the stained sections were scanned at 40x magnification using a Leica Aperio® slide scanner and the results assessed employing the local ImageScope (version 12.3.2.1813) for staining quality assessment and the linked online eSlide Manager (version 12.1.0.5029) for digital analysis.

The region of periprostatic adipose tissue (PPAT) was manually selected from different periprostatic regions. An experienced pathologist (SF) reviewed histopathology reviewed histopathology and guided selection of regions specifically but not exclusively around tumour within the prostate gland. We did not include damaged adipose tissue at section edges, blood vessels, and artefacts. The selected total area on each slide was not less than $30,000\mu m^2$. Following standardised parameters, we used the Leica Aperio Positive Pixel Count algorithm to quantify the positive and negative staining of 3,3'-diaminobenzidine (DAB) and Hematoxylin (counterstain), respectively (**Figure 1**). The algorithm automatically analysed the positive DAB staining of the selected regions into three different coloured pixels: strong positive (Sp) (red), positive (p) (orange), and weak positive (Wp) (yellow). The Hematoxylin

counterstain was represented by blue negative pixels. At the same time, the positivity (%) was calculated [Positivity (%) = (Wp + p + Sp) / N_{total} x 100] (**Figure 2**), where N_{total} is the total number of positive and negative pixels in the selected regions. The positivity (%) represents the concentration of the protein in PPAT.

Reproducibility of the slide digital analysis was assessed in a subgroup of 14 randomly selected patients by repeated measures in two-week intervals. An excellent interrater reliability was shown with an intraclass correlation coefficient of 0.951 in single measures ($p < 0.001$).

2.4   MRI technique

The full MRI protocol is detailed elsewhere [4]. PFV was determined using a semi-automated segmentation technique on contiguous T_1-weighted axial MRI slices from the level of the prostate base to the apex. PFV was normalised to prostate volume (PV) to account for variations in PV (NPFV=PFV/PV). High-resolution T2 weighted scans and apparent diffusion coefficient (ADC) maps derived from diffusion weighted imaging (DWI) were used for identification of the index PCa lesion by an experienced uroradiologist. Subsequently, in 48 patients who underwent dynamic contrast enhancement, quantitative parameters (K_{trans} and K_{ep}) were extracted with OleaSphere software version 3.0 (Olea Medical, La Ciotat, France).

2.5   Statistical Analyses

Patients were stratified into three groups according to the Gleason score of the final prostatectomy specimen: ≤6, 7(3+4) and 7(4+3) or more. The association between the three groups and adipokine expression levels including AR and clinical and pathological data was determined using Kruskal-Wallis and one-way analysis of variance (ANOVA) tests for parametric and non-parametric continuous variables, respectively, and Chi-square test for

categorical variables (WHO weight classification, pT stage and D'Amico risk classification). Receiver Operating Characteristic (ROC) curve analysis was used to test the ability of TNFα and VEGF to differentiate between high-grade (GS ≥ 7) and low-grade (GS ≤ 6) prostate cancers. Binary logistic regression analysis was used to establish an independent effect of TNFα and VEGF on high-grade (GS ≥ 7) vs low-grade (GS ≤ 6) prostate cancers. Independent sample t-test was used to compare the adipokine levels, AR, functional MRI quantitative values (K_{trans}, K_{ep}, and ADC value) and age with pT and GS upgrading from biopsy specimen to RP. Spearman correlation coefficients (ρ) were used to evaluate the relationship between the adipokine levels (TNFα and VEGF), AR, MRI parameters (K_{trans}, K_{ep}, and ADC value), NPFV and pre- and post-operative GS. *p* value of < 0.05 was considered statistically significant. IBM Statistical Package for the Social Sciences (SPSS) (version 23) for OS X was used for data analyses.

3 Results

The mean age of the cohort (N=69) was 66.13 ± 5.47 years (range, 53-78), and the mean BMI was 28.12 ± 4.37 kg/m^2 (range, 20.5 - 40.6). According to WHO classification, 17 patients were classified as normal weight (27.86 %), 27 as overweight (44.26%), 13 as obese class I (21.31 %), three as obese class II (4.93 %), and 1 as obese class III (1.64%). **Table 1** summarises the patients' characteristics categorised into three groups according to the post-operative GS based on histopathology.

The mean ranks of the positivity of vascular endothelial growth factor (VEGF) and tumour necrosis alpha (TNFα) were statistically different between the three groups (GS ≤ 6, GS = 7(3+4) and GS ≥ 7(4+3), with [H (2) = 11.038, p = 0.004] and [H (2) = 13.086, p = 0.001], respectively (**Figure 3**). There were no differences in the mean ranks of immunopositivity for AR between the three groups [H (2) = 1.388, p = 0.5], nor in mean age [H (2) = 1.880, p = 0.391] (**Table 1**).

After dichotomisation of PCa histopathology into low (GS ≤ 6) and high (GS ≥ 7) grade groups, ROC curve analysis yielded areas under the curves for TNFα and VEGF of 0.897 (p = 0.001) and 0.910 (p = 0.001), with Youden's indices of 9.03 and 4.22, respectively. Use of these cut-offs provided a sensitivity and specificity for differentiating between low and high-grade cancers of 74.6% and 100%, respectively for TNFα and 85.7% and 100%, respectively for VEGF (**Figure 4**).

Binary logistic regression analysis showed that both TNFα and VEGF could predict the risk of having high-grade PCa (GS ≥ 7), with odds ratios (OR) of 1.343 (95% CI, 1.01-1.79; p = .043) and 1.921 (95% CI, 1.11-3.33; p = .02), respectively. A Hosmer-Lemeshow test revealed that the data fit the model well [$\chi 2(8)$ = 1.81, p = 0.986].

Patients with stage pT$_3$ had statistically significantly higher positivity of TNFα (18.2 ± 8.95) than patients with stage pT$_2$ (13.27 ± 10.66), t (67) = -2.03, p = 0.047. There was no relationship between AR and VEGF and pT stage of PCa, [t (67) = .458, p = 0.649] and [t (67) = -.547, p = 0.586], respectively).

Mean expression levels of TNFα and VEGF for Gleason score ≤ 6 disease were 4.1 (± 3.7) and 2.8 (±1.1) respectively. In contrast mean levels of expression for TNFα and VEGF for Gleason score 7 and more disease were 15.4 (±9.7) and 15.1 (±11.3) respectively. There were 22 (31.8%) patients with upgraded GS from biopsy specimen to final RP (14 had Gleason score 6 disease on biopsies and were upgraded to GS 7 or more). Analysis of 20 radical prostatectomy cases (20/69; 28.9%) diagnosed with Gleason 6 on biopsies showed that 70% (14/20; 70%) were upgrade to Gleason 7 or more on final histopathology. Performance of expression level analysis for TNF α and VEGF in those with upgraded disease vs. non-upgraded disease showed statistically significant differences (**Table 2**). VEGF expression between the non-upgraded (2.83 ± 1.18; n = 6) and upgraded (6.85 ± 3.45; n = 14) groups was statistically significant [t (18) = -2.75, p = 0.013]. Similarly, there was a difference in the mean of TNF α expression between the non-upgraded (4.11 ± 3.77; n = 6) and upgraded (10.55 ± 8; n = 14) groups with statistically significance [t (18) = -1.86, p = 0.039]. This suggests a high expression of TNFα and VEGF in presence of low grade disease on biopsy may indicate presence of high grade disease in the prostate.

Immunohistochemical expression of TNFα was significantly positively correlated with K$_{trans}$ (ρ = 0.327, p = 0.023), but not with K$_{ep}$ (ρ = 0.162, p = 0.270) or ADC value (ρ = -0.096, p = 0.516). There was no significant correlation between VEGF expressions with any of quantitative MRI parameters. **Table 3** summarises the correlations results.

4 Discussion

To our knowledge, this is the first study to investigate the relationship between the inflammatory and angiogenic adipokine (TNFα and VEGF) expression levels in PPAT and the aggressivity of PCa by comparing their immunohistochemical expression with Gleason scores (GS), pathological tumour staging (pT), and quantifiable MR imaging biomarkers. The results indicate a strong correlation between PPAT TNFα positivity and histopathological GS, as well as pT stage. We observed that both TNFα and VEGF were significant correlating with the risk of having high-grade PCa (GS $\geq$ 7) following RP. However, PPAT androgen receptor expression had no relationship with either post-operative GS or pT stage. It is, however interesting to observe that men who were upgraded from low GS on biopsy had statistically significant different level of expression for both TNFα and VEGF to those who continued to have low grade disease with similar GS on biopsy and radical prostatectomy histology.

Recent studies [1, 3, 29-31], including our previous study [4], have confirmed the relationship between the adiposity of periprostatic fat and the aggressivity of PCa. The cross-talk between PPAT and PCa cells could modify the phenotype and characteristics of closely related adipocytes, which can become more metabolically active adipocytes called "cancer-associated adipocytes" [11, 12]. These cells can stimulate and support PCa progression by releasing FFA, the major source of PCa energy, through lipolysis and secreting adipokines that stimulate tumour progression through a paracrine effect [12, 32]. This may suggest that both adiposity and adipokine activity of periprostatic fat have an impact on the aggressivity of PCa. However, at present, imaging is unable to assess adipokine activity of periprostatic fat. Interestingly, BMI, the marker of generalised obesity, has no relationship with NPFV nor PCa aggressiveness indicating that periprostatic fat adiposity is more important than BMI [4].

TNFα is a pro-inflammatory and lipolytic adipokine that induces apoptosis and inhibits carbohydrate metabolism and adipogenesis [33-37]. Serum TNFα has been reported as a biomarker for PCa diagnosis [20]. As a pro-inflammatory cytokine, it can influence PCa progression and increase the risk of metastasis [19, 23, 24]. Focusing on PPAT, a study showed that inflammation was associated with high-grade PCa [14]. PPAT TNFα is higher in obese men, which contributes to insulin resistance [9, 35, 38-40], but it is not associated with lipolysis in cachectic patients with gastrointestinal cancers [36]. Ribeiro et al [41] have reported that TNFα was expressed by approximately 1.7-fold higher in PPAT explants stimulated with a PC3 human PCa cell line conditioned medium, but not by stromal vascular fractions that did not contain mature adipocytes, suggesting that mature PPAT adipocytes, the cancer-associated adipocytes, can significantly crosstalk with PCa cells and secrete larger amount of TNFα [11]. Therefore, we investigated its relation to PCa grading along with staging and found that it was significantly correlated with the both.

K_{trans}, representing the rate of accumulation of gadolinium-based contrast agent in the extravascular extracellular space, is a measure of capillary permeability. Our study showed that K_{trans} in the primary lesion was significantly correlated with PPAT TNFα but not to PPAT VEGF. This may reflect the consequence of the inflammatory response of PPAT and increased vascular permeability leading to transfer of the contrast agent from blood vessels to the extracellular matrix. It has been reported that PPAT angiogenesis may facilitate seeding of a PCa microenvironment with adipocyte precursors (lipoblasts) [42]. These lipoblasts secrete numerous factors (e.g. IL-6 and TNFα) involved in the inflammatory response, particularly in obesity [25]. Taking all of this into consideration, there is a clear implication that TNFα has a significant role as a pro-inflammatory adipokine, secreted by activated mature PPAT adipocytes, together with the angiogenic PPAT VEGF, creating a favourable stromal

microenvironment that promotes PCa progression by inducing vascularity and increasing vascular permeability [43-50], which facilitates seeding PPAT lipoblasts to the PCa tumour stromal microenvironment [42]. Moreover, as a lipolytic factor, PPAT TNFα may increase the release of FFA, which has been found to be the major source of PCa energy[32]. The quantitative K*trans* of primary prostate lesion could provide an estimate of angiogenic activity of periprostatic fat, however this needs further research.

Our results showed that both TNFα and VEGF positivity at IHC can distinguish between low (GS ≤ 6) and high (GS ≥ 7) grade PCa. TNFα and VEGF expression levels above 9.03% and 4.22% had a 74.6% and 85.7% chance of having high-grade PCa, respectively. These findings have strong clinical implications, if externally validated to predict upgrading from GS biopsy to RP, the practical utility of measuring the expression of TNFα and VEGF in the periprostatic fat sample during prostate biopsy could be realised, and the level of expression for both could become a marketable test, similar to Oncotype DX, Prolaris, and Decipher tests, that predict upgrading and help in decision-making such as in active surveillance versus radical treatment [51].

Androgens upregulate the adrenoreceptors of catecholamines in adipose tissue, and their receptors are more prominent in visceral fat than subcutaneous fat [52, 53]. This may indicate the uptake of the lipolytic catecholamines in visceral fat is higher, leading to the release of greater amounts of FFA, the major source of PCa energy [32, 52, 53]. Therefore, we included PPAT AR in our analysis, but did not find any correlation with GS or pT stage.

There are some limitations to our study. The present investigation was a single centre cohort and the results require further validation through a multicentre design. Quantitative MRI data was available for only 48 cases in the cohort (we had no imaging data for the remaining 21 cases as they were scanned on 1.5T MRI). Though we demonstrated no correlation between

PPAT VEGF and K_{trans} of the primary lesion at MRI, a larger sample size might have altered this result. Although we had only 6 patients in Gleason score 6 diseases, trends do suggest that periprostatic fat biopsies at the time of prostatic biopsy for immunostaining for inflammatory biomarkers could represent a time-saving way of obtaining useful information and predicting aggressive PCa.

In conclusion, PPAT TNFα and VEGF immunostaining was significantly positively correlated with the aggressivity of PCa (grade and stage) in men undergoing radical prostatectomy for clinically localised disease. As PCa biomarkers, PPAT metabolic activity measured by immunohistochemical expression of TNFα and VEGF significantly correlates with the risk of having high-grade prostate cancer disease including upgradation from prostate biopsy results.

5 Acknowledgements

Conflicts of interest:

None.

References

1. Bhindi B, Trottier G, Elharram M, Fernandes K, Lockwood G, Toi A, Hersey K, Finelli A, Evans A, van Der Kwast T *et al*: **Measurement of peri-prostatic fat thickness using transrectal ultrasonography (TRUS): a new risk factor for prostate cancer**. *BJU Int* 2012, **110**(7):980-986.

2. Van Roermund JGH, Hinnen KA, Tolman CJ, Bol GH, Witjes JA, Bosch JLHR, Kiemeney LA, van Vulpen M: **Periprostatic fat correlates with tumour aggressiveness in prostate cancer patients**. *Bju International* 2010, **107**:1775-1779.

3. Woo S, Cho JY, Kim SY, Kim SH: **Periprostatic Fat Thickness on MRI: Correlation With Gleason Score in Prostate Cancer**. *American Journal of Roentgenology* 2015, **204**:W43-W47.

4. Dahran N, Szewczyk-Bieda M, Wei C, Vinnicombe S, Nabi G: **Normalized periprostatic fat MRI measurements can predict prostate cancer aggressiveness in men undergoing radical prostatectomy for clinically localised disease**. *Scientific Reports* 2017, **7**(1):4630.

5. Waki H, Tontonoz P: **Endocrine functions of adipose tissue**. *Annu Rev Pathol* 2007, **2**:31-56.

6. Bastard JP, Feve B: **The secretory face of the adipose cell: a tribute to two queens, leptin and adiponectin**. *Biochimie* 2012, **94**(10):2063-2064.

7. Paz-Filho G, Lim EL, Wong ML, Licinio J: **Associations between adipokines and obesity-related cancer**. *Front Biosci (Landmark Ed)* 2011, **16**:1634-1650.

8. Powell K: **Obesity: the two faces of fat**. *Nature* 2007, **447**(7144):525.

9. Weisberg SP, McCann D, Desai M, Rosenbaum M, Leibel RL, Ferrante AW, Jr.: **Obesity is associated with macrophage accumulation in adipose tissue**. *J Clin Invest* 2003, **112**(12):1796-1808.

10. Bastard JP, Maachi M, Lagathu C, Kim MJ, Caron M, Vidal H, Capeau J, Feve B: **Recent advances in the relationship between obesity, inflammation, and insulin resistance**. *Eur Cytokine Netw* 2006, **17**(1):4-12.

11. Muller C: **Tumour-surrounding adipocytes are active players in breast cancer progression**. *Ann Endocrinol (Paris)* 2013, **74**:108-110.

12. Nieman KM, Romero IL, Lengyel E, Van Houten B: **Adipose tissue and adipocytes support tumorigenesis and metastasis**. *Biochimica et Biophysica Acta - Molecular and Cell Biology of Lipids* 2013.

13. Laurent V, Guérard A, Mazerolles C, Le Gonidec S, Toulet A, Nieto L, Zaidi F, Majed B, Garandeau D, Socrier Y *et al*: **Periprostatic adipocytes act as a driving force for prostate cancer progression in obesity**. 2016, **7**:10230.

14. Gucalp A, Iyengar NM, Zhou XK, Giri DD, Falcone DJ, Wang H, Williams S, Krasne MD, Yaghnam I, Kunzel B *et al*: **Periprostatic adipose inflammation is associated with high-grade prostate cancer**. *Prostate Cancer Prostatic Dis* 2017.

15. Hube F, Hauner H: **The role of TNF-alpha in human adipose tissue: prevention of weight gain at the expense of insulin resistance?** *Horm Metab Res* 1999, **31**(12):626-631.

16. Roskoski R, Jr.: **Vascular endothelial growth factor (VEGF) and VEGF receptor inhibitors in the treatment of renal cell carcinomas**. *Pharmacol Res* 2017, **120**:116-132.

17. Rutkowski JM, Davis KE, Scherer PE: **Mechanisms of obesity and related pathologies: The macro? and microcirculation of adipose tissue**. In., vol. 276. Oxford, UK; 2009: 5738-5746.

18. Di Alberti L, Rossetto A, Albanese M, D'Agostino A, De Santis D, Bertossi D, Nocini PF: **Expression of Vascular Endothelial Growth Factor (VEGF) mRNA in healthy bone tissue around implants and in peri-implantitis**. *Minerva Stomatol* 2013.

19. Grivennikov SI, Greten FR, Karin M: **Immunity, inflammation, and cancer**. *Cell* 2010, **140**(6):883-899.

20. Chadha KC, Miller A, Nair BB, Schwartz SA, Trump DL, Underwood W: **New serum biomarkers for prostate cancer diagnosis**. *Clin Cancer Investig J* 2014, **3**(1):72-79.

21. Khandekar MJ, Cohen P, Spiegelman BM: **Molecular mechanisms of cancer development in obesity**. *Nat Rev Cancer* 2011, **11**(12):886-895.

22. Roskoski R, Jr.: **Vascular endothelial growth factor (VEGF) signaling in tumor progression**. *Crit Rev Oncol Hematol* 2007, **62**(3):179-213.

23. Sethi G, Sung B, Aggarwal BB: **TNF: a master switch for inflammation to cancer**. *Front Biosci* 2008, **13**:5094-5107.

24. Szlosarek P, Charles KA, Balkwill FR: **Tumour necrosis factor-α as a tumour promoter**. *European Journal of Cancer* 2006, **42**(6):745-750.

25. Cousin B, Munoz O, Andre M, Fontanilles A, Dani C, Cousin J, Laharrague P, Casteilla L, Penicaud L: **A role for preadipocytes as macrophage-like cells**. *Faseb J* 1999, **13**(2):305-312.

26. Zhang J, Li H, Wang X, Qi H, Miao X, Zhang T, Chen G, Wang M: **Phage-derived fully human antibody scFv fragment directed against human vascular endothelial growth factor receptor 2 blocked its interaction with VEGF**. *Biotechnol Prog* 2012, **28**(4):981-989.

27. Ribeiro R, Monteiro C, Silvestre R, Castela A, Coutinho H, Fraga A, Príncipe P, Lobato C, Costa C, Cordeiro-da-Silva A *et al*: **Human periprostatic white adipose tissue is rich in stromal progenitor cells and a potential source of prostate tumor stroma**. *Experimental Biology and Medicine* 2012, **237**(10):1155-1162.

28. Cao Y: **Angiogenesis in Adipose Tissue**. New York, NY: New York, NY : Springer New York : Imprint: Springer; 2013.

29. Van Roermund JG, Bol GH, Witjes JA, Ruud Bosch JL, Kiemeney LA, van Vulpen M: **Periprostatic fat measured on computed tomography as a marker for prostate cancer aggressiveness**. *World J Urol* 2009, **28**:699-704.

30. Zhang Q, Sun LJ, Qi J, Yang ZG, Huang T, Huo RC: **Periprostatic adiposity measured on magnetic resonance imaging correlates with prostate cancer aggressiveness**. *Urol J* 2014, **11**(4):1793-1799.

31. Tan WP, Lin C, Chen M, Deane LA: **Periprostatic Fat: A Risk Factor for Prostate Cancer?** *Urology* 2016, **98**:107-112.

32. Liu Y: **Fatty acid oxidation is a dominant bioenergetic pathway in prostate cancer**. *Prostate Cancer and Prostatic Diseases* 2006, **9**(3):230-234.

33. Prins JB, Niesler CU, Winterford CM, Bright NA, Siddle K, O'Rahilly S, Walker NI, Cameron DP: **Tumor necrosis factor-alpha induces apoptosis of human adipose cells**. *Diabetes* 1997, **46**(12):1939-1944.

34. Wellen KE, Hotamisligil GS: **Inflammation, stress, and diabetes**. *J Clin Invest* 2005, **115**(5):1111-1119.

35. Cawthorn WP, Sethi JK: **TNF-α and adipocyte biology**. *FEBS letters* 2008, **582**(1):117-131.

36. Rydén M, Agustsson T, Laurencikiene J, Britton T, Sjölin E, Isaksson B, Permert J, Arner P: **Lipolysis—Not inflammation, cell death, or lipogenesis—Is involved in adipose tissue loss in cancer cachexia**. *Cancer* 2008, **113**(7):1695-1704.

37. Ouchi N, Parker JL, Lugus JJ, Walsh K: **Adipokines in inflammation and metabolic disease**. *Nat Rev Immunol* 2011, **11**(2):85-97.

38. Xu H, Barnes GT, Yang Q, Tan G, Yang D, Chou CJ, Sole J, Nichols A, Ross JS, Tartaglia LA *et al*: **Chronic inflammation in fat plays a crucial role in the development of obesity-related insulin resistance**. *J Clin Invest* 2003, **112**(12):1821-1830.

39. Heilbronn LK, Campbell LV: **Adipose tissue macrophages, low grade inflammation and insulin resistance in human obesity**. *Curr Pharm Des* 2008, **14**(12):1225-1230.

40. Olefsky JM, Glass CK: **Macrophages, inflammation, and insulin resistance**. *Annu Rev Physiol* 2010, **72**:219-246.

41. Ribeiro, Ricardo J T, Monteiro, Cátia P D, Cunha, Virginia F P M, Azevedo, Andreia S M, Oliveira, Maria J, Monteiro, Rosário, Fraga, Avelino M, Príncipe, Paulo, Lobato, Carlos, Lobo, Francisco, Morais, António, Silva, Vitor, Sanches-Magalhães, José, Oliveira, Jorge, Guimarães, João T, Lopes, Carlos M S, and Medeiros, Rui M. **Tumor Cell-educated Periprostatic Adipose Tissue Acquires an Aggressive Cancer-promoting Secretory Profile.** Cellular Physiology and Biochemistry : *International Journal of Experimental Cellular Physiology, Biochemistry, and Pharmacology* 2012, **29**:233-40.

42. Zhang Y, Daquinag AC, Amaya-Manzanares F, Sirin O, Tseng C, Kolonin MG: **Stromal progenitor cells from endogenous adipose tissue contribute to pericytes and adipocytes that populate the tumor microenvironment**. *Cancer research* 2012, **72**(20):5198.

43. Ito A, Hirota S, Mizuno H, Kawasaki Y, Takemura T, Nishiura T, Kanakura Y, Katayama Y, Nomura S, Kitamura Y: **Expression of vascular permeability factor (VPF/VEGF) messenger RNA by plasma cells: possible involvement in the development of edema in chronic inflammation**. *Pathol Int* 1995, **45**(10):715-720.

44. Claffey KP, Brown LF, del Aguila LF, Tognazzi K, Yeo KT, Manseau EJ, Dvorak HF: **Expression of vascular permeability factor/vascular endothelial growth factor by melanoma cells increases tumor growth, angiogenesis, and experimental metastasis**. *Cancer Res* 1996, **56**(1):172-181.

45. Kalkanis SN, Carroll RS, Zhang J, Zamani AA, Black PM: **Correlation of vascular endothelial growth factor messenger RNA expression with peritumoral vasogenic cerebral edema in meningiomas**. *J Neurosurg* 1996, **85**(6):1095-1101.

46. Sasaki R: [**Microvessel count and vascular endothelial growth factor in renal cell carcinoma**]. *Nihon Hinyokika Gakkai Zasshi* 1996, **87**(8):1032-1040.

47. Viglietto G, Romano A, Maglione D, Rambaldi M, Paoletti I, Lago CT, Califano D, Monaco C, Mineo A, Santelli G *et al*: **Neovascularization in human germ cell tumors correlates with a marked increase in the expression of the vascular endothelial growth factor but not the placenta-derived growth factor**. *Oncogene* 1996, **13**(3):577-587.

48. Takano S, Yoshii Y, Kondo S, Suzuki H, Maruno T, Shirai S, Nose T: **Concentration of vascular endothelial growth factor in the serum and tumor tissue of brain tumor patients**. *Cancer Res* 1996, **56**(9):2185-2190.

49. Saito W, Kase S, Fujiya A, Dong Z, Noda K, Ishida S: **Expression of vascular endothelial growth factor and intravitreal anti-VEGF therapy with bevacizumab in vasoproliferative retinal tumors**. *Retina* 2013, **33**(9):1959-1967.

50. Wang W, Merrill MJ, Borchardt RT: **Vascular endothelial growth factor affects permeability of brain microvessel endothelial cells in vitro**. *Am J Physiol* 1996, **271**(6 Pt 1):C1973-1980.

51. Wei, Wang, Lampert, Schlanger, Depriest, Hu, Gomez, Murakam, Glenn, Conroy, Morrison, Azabdaftari, Mohler, Liu, and Heemers. **Intratumoral and Intertumoral Genomic Heterogeneity of Multifocal Localized Prostate Cancer Impacts**

Molecular Classifications and Genomic Prognosticators. *Eur Urol* 2017, **71**(2): 183-92.

52. Lee J: **Adipose tissue macrophages in the development of obesity-induced inflammation, insulin resistance and type 2 diabetes**. *Arch Pharm Res* 2013, **36**(2):208-222.

53. Ibrahim MM: **Subcutaneous and visceral adipose tissue: structural and functional differences**. In., vol. 11. Oxford, UK; 2010: 11-18.
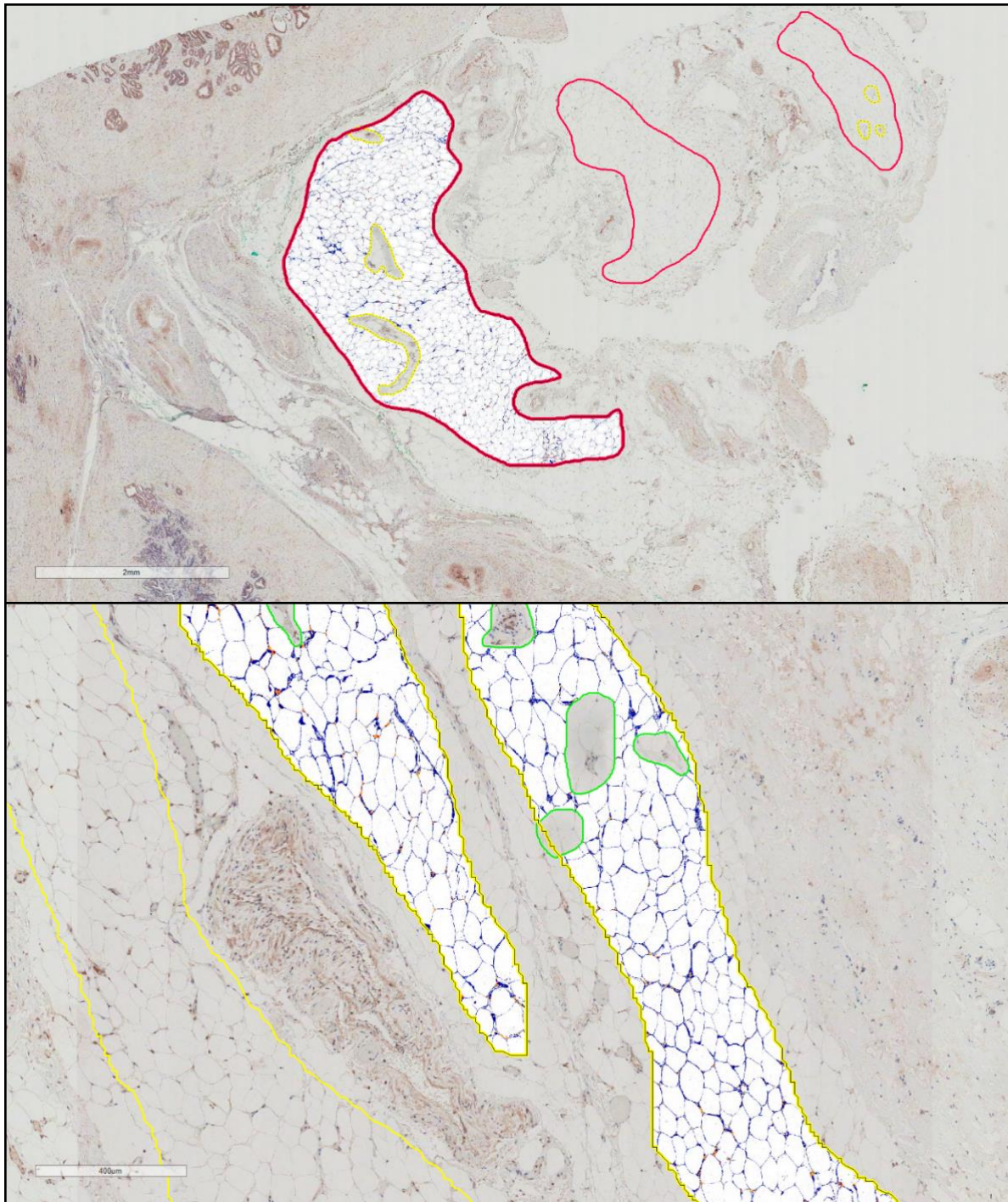
Figure 1: (I) Periprostatic adipose tissues were manually selected from multiple areas proximal and distal to the prostate tissue (red marks). The Positive Pixel Count algorithm was used to quantify the positive and negative staining within the selected regions. (II) A closer view of the net-shaped adipose tissue analysed by the Positive Pixel Count algorithm. Lipid droplets were not included in the analysis. Artefacts, blood vessels, and other types of tissues within the selected regions were manually excluded (green marks).
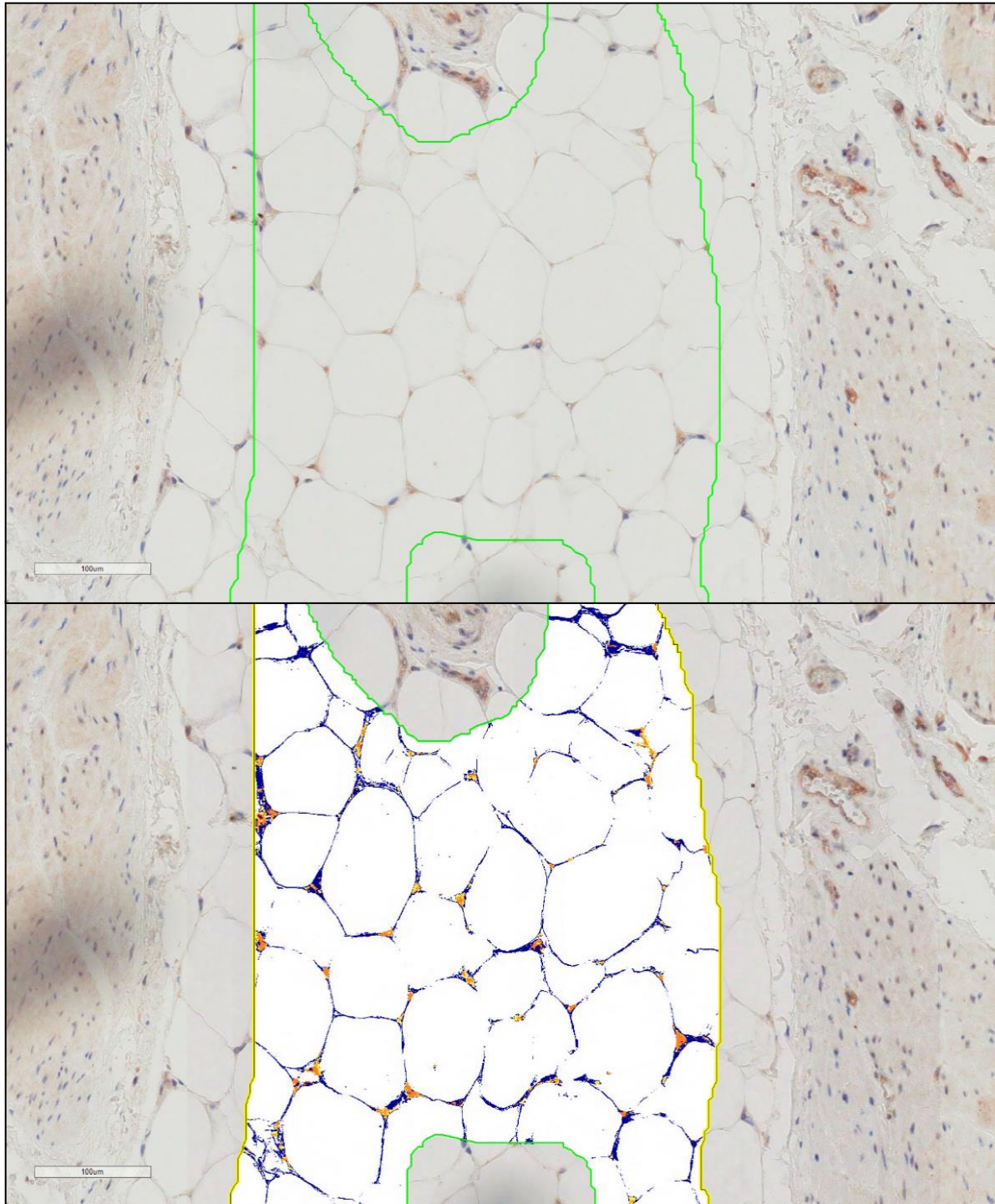
Figure 2: (I) Manually selected periprostatic adipose tissue before analysis. (II) After running the Positive Pixel Count algorithm, the positive DAB staining (I) of the selected region was divided into 3 different coloured pixels (yellow for weak positive; orange for positive; red for strong positive) based on standardised levels of intensity (the concentration of DAB staining). The Hematoxylin counterstain was represented by blue negative pixels. The positivity (%) was calculated by dividing the number of positive pixels by the total pixel count within the selected region and multiplying by 100.
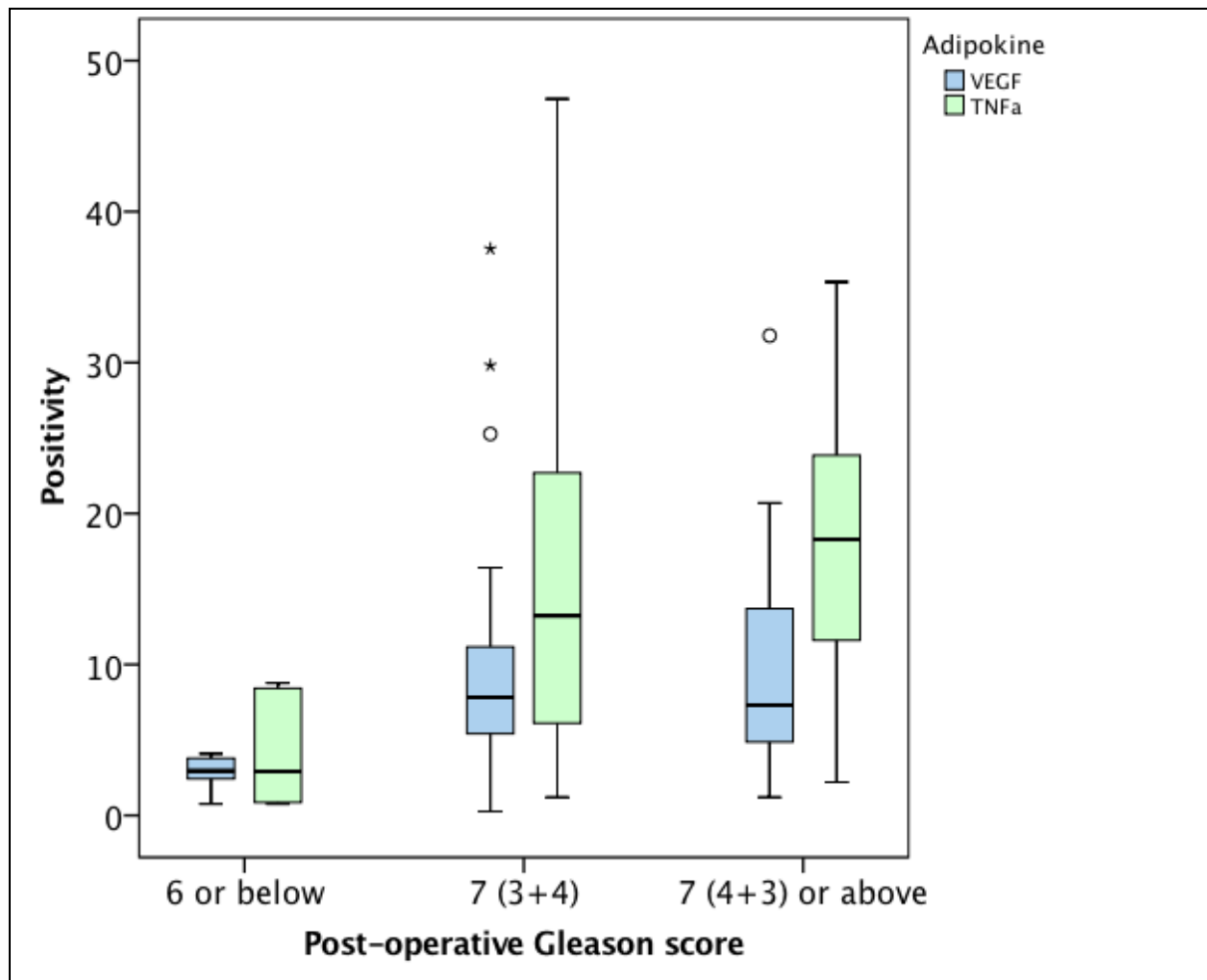
Figure 3: Box plot showing the differences in the distribution and the median of the positivity of vascular endothelial growth factor (VEGF) and tumour necrosis factor alpha (TNFa) in the three groups stratified according to post-operative Gleason score.
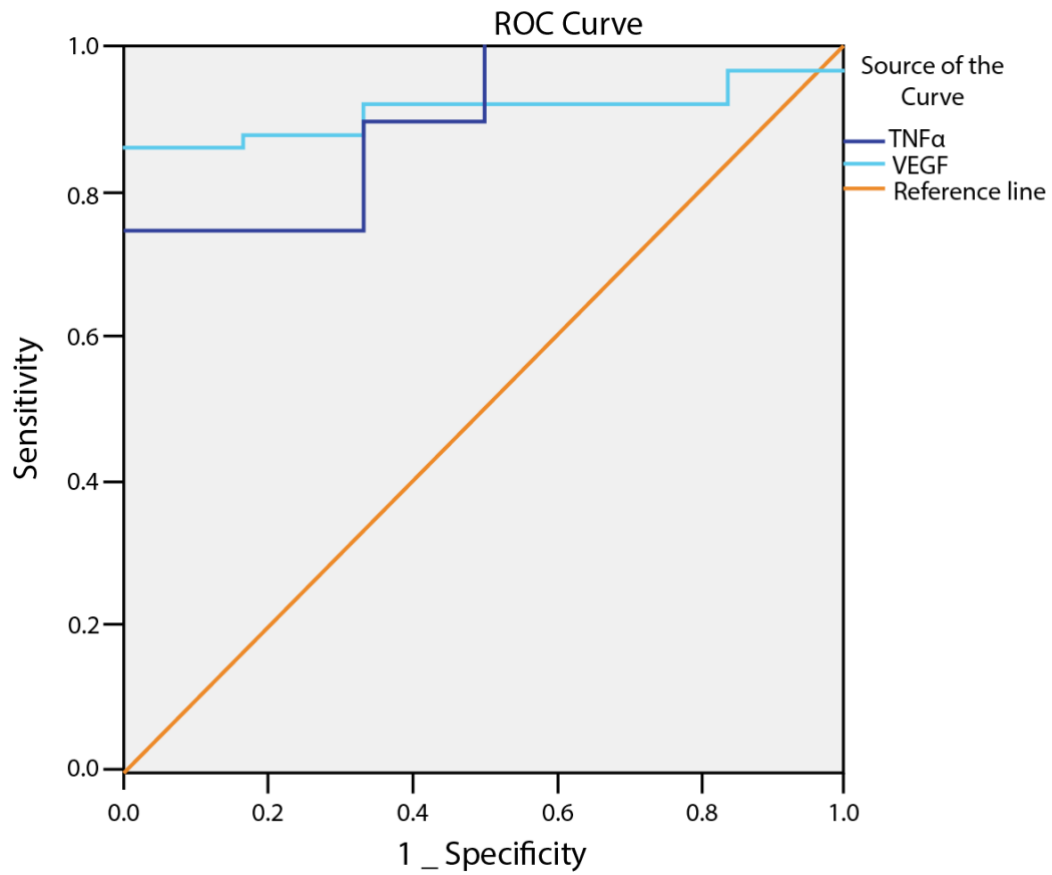
Figure 4: ROC curve showing the areas under the curves of tumour necrosis factor alpha (TNFa; green line) and vascular endothelial growth factor (VEGF; blue line).

Table 1: Patient characteristics.

	Group 1 Post-operative Gleason score ≤6	Group 2 Post-operative Gleason score 7 (3+4)	Group 3 Post-operative Gleason score 7 (4+3) and over	*p* value
Mean ± Standard Deviation				
No.	$n = 6$	$n = 35$	$n = 28$	
Age	64 ± 8.17	65.83 ± 5.67	66.96 ± 4.54	.391[a]
VEGF (%)	2.83 ± 1.18	10.03 ± 7.74	9.45 ± 6.65	**.004[b]**
AR (%)	7.44 ± 5.07	5.64 ± 3.71	7.15 ± 5.96	.500[b]
TNFa (%)	4.1 ± 3.77	14.89 ± 10.76	18.32 ± 8.75	**.001[b]**
Initial PSA (ng/ml)	7.9 ± 2.13	10.69 ± 7.53	11.53 ± 6.39	.317[b]
PV (cm^3)	64.64 ± 8.74	48.99 ± 26.035	55.44 ± 23.01	.165[b]
WHO classification *N* (%)*				
No.	$n = 4$	$n = 33$	$n = 24$	
Normal weight	1 (25)	10 (30.3)	6 (25)	
Overweight	3 (75)	16 (48.5)	8 (33.3)	
Obesity class I	0	5 (15.2)	8 (33.3)	.568[c]
Obesity class II	0	2 (6.1)	1 (4.2)	
Obesity class III	0	0	1 (4.2)	
Pathological stage *N* (%)*				
No.	$n = 6$	$n = 35$	$n = 28$	
T$_2$	5 (83.3)	24 (68.6)	11 (39.3)	**.027[c]**
T$_3$	1(16.7)	11 (31.4)	17 (60.7)	
D'Amico risk classification *N* (%)*				
No.	$n = 6$	$n = 35$	$n = 28$	
Low	5 (83.3)	9 (25.7)	1 (3.6)	
Intermediate	1 (16.7)	17 (48.6)	10 (35.7)	**<.001[c]**
High	0	9 (25.7)	17 (60.7)	

VEGF = Vascular endothelial growth factor; AR = Androgen receptors; TNFa = Tumour necrosis factor alpha; PSA = Prostate specific antigen; PV = Prostate volume.
Patients were stratified according to post-operative Gleason score
[a]ANOVA, [b]Kruskal-Wallis test, [c]χ^2 test
*(%) within each group
p value is significant <0.05

Table 2. Independent-sample t test was used to compare the differences in the mean adipokine Immunopositivity (%) for upgraded and not upgraded from low-grade (GS = 3+3) PCa at biopsy ($n = 20$).

		N	Mean (%)	Std. Deviation (%)	Std. Error Mean (%)	t	$^*p$ value
VEGF	not upgraded	6	2.83	1.18	.48	-2.75	.013
	upgraded	14	6.85	3.45	.92		
TNFa	not upgraded	6	4.11	3.77	1.53	-1.86	.079
	upgraded	14	10.55	8	2.14		

(%) immunopositivity within each group

Table 3: The relationship between periprostatic adipose tissue adipokines (VEGF and TNFa), androgen receptors, age, prostate volume, Quantitative values of functional MRIs (DCE-MRI and DWI), fat measures, body mass index (BMI), prostate specific antigen (PSA) and pre- and post-operative Gleason scores using Spearman correlation coefficient.

			AR	VEGF	TNFa	Age	PV	AFA	SFT	PSA	BMI	K_{trans}	K_{ep}	ADC	NPFV	Post-op GS	Biopsy GS
Spearman's rho	AR	Correlation Coefficient	1.000	.269*	.226	.190	.057	.112	.062	.101	.107	.194	.084	.302*	.018	.045	.103
		Sig. (2-tailed)	.	.025	.062	.119	.653	.383	.629	.408	.411	.185	.572	.037	.886	.714	.399
		N	69	69	69	69	64	63	63	69	61	48	48	48	64	69	69
	VEGF	Correlation Coefficient	.269*	1.000	.475**	.009	-.143	.040	.127	.175	.110	.158	.118	.012	.068	.190	.265*
		Sig. (2-tailed)	.025	.	.000	.943	.259	.757	.320	.151	.397	.284	.426	.933	.595	.117	.028
		N	69	69	69	69	64	63	63	69	61	48	48	48	64	69	69
	TNFa	Correlation Coefficient	.226	.475**	1.000	-.012	-.038	.156	.278*	.177	.233	.327*	.162	-.096	.082	.345**	.419**
		Sig. (2-tailed)	.062	.000	.	.921	.767	.223	.027	.146	.070	.023	.270	.516	.517	.004	.000
		N	69	69	69	69	64	63	63	69	61	48	48	48	64	69	69
	K_{trans}	Correlation Coefficient	.194	.158	.327*	.126	.159	.070	.089	.060	.115	1.000	.682**	.081	.157	.005	.110
		Sig. (2-tailed)	.185	.284	.023	.395	.281	.640	.551	.687	.443	.	.000	.588	.286	.974	.458
		N	48	48	48	48	48	47	47	48	47	48	48	47	48	48	48
	K_{ep}	Correlation Coefficient	.084	.118	.162	.032	.211	-.106	.061	.011	.051	.682**	1.000	.122	.057	-.123	.054
		Sig. (2-tailed)	.572	.426	.270	.828	.150	.480	.683	.941	.735	.000	.	.413	.701	.405	.716
		N	48	48	48	48	48	47	47	48	47	48	48	47	48	48	48
	ADC	Correlation Coefficient	.302*	.012	-.096	.067	-.068	-.221	-.334*	-.230	-.365*	.081	.122	1.000	-.163	-.473**	-.361*
		Sig. (2-tailed)	.037	.933	.516	.651	.644	.136	.022	.116	.012	.588	.413	.	.268	.001	.012
		N	48	48	48	48	48	47	47	48	47	47	47	48	48	48	48

AR = Androgen receptors; VEGF = Vascular endothelial growth factor; TNFa = Tumour necrosis factor alpha; PV = Prostate volume; AFA = Abdominal fat area; SFT = Subcutaneous fat thickness; PSA = Prostate specific antigen; BMI = Body mass index; K_{trans} = Transfer constant; K_{ep} = Reverse reflux rate constant; ADC = Apparent diffusion coefficient; NPFV = Normalised periprostatic fat volume; GS = Gleason score.

*. Correlation is significant at the 0.05 level (2-tailed).

**. Correlation is significant at the 0.01 level (2-tailed).
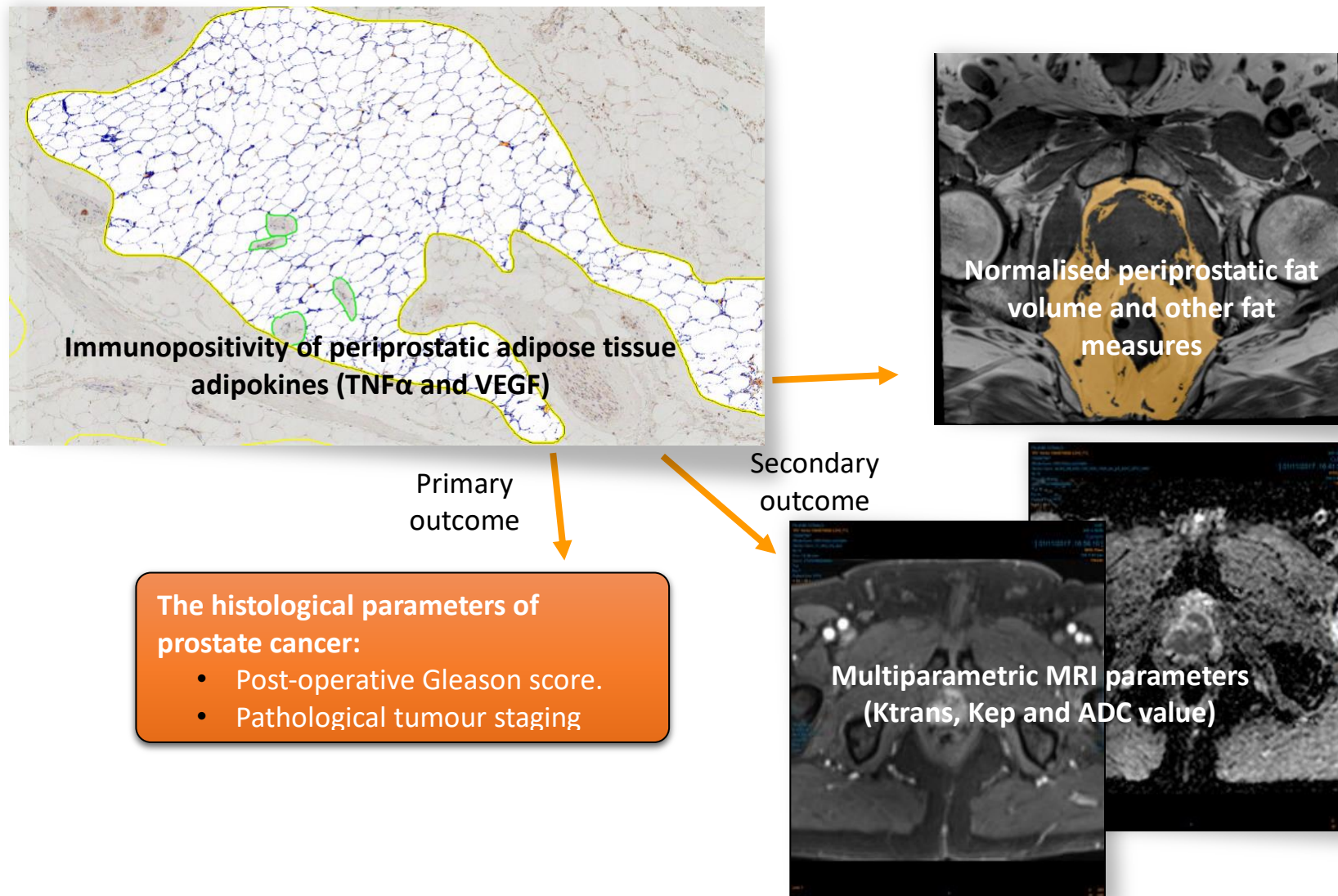
Figure S1: Schematic diagram showing the primary and secondary outcomes of this study.

Table S1: Power analysis.

Fat measures	Effect Size (f)	α error probability	Power (1-β error probability)	Sample size calculated	*p* value[a]
AR	.46	.05	.8	51	.249
VEGF	.64	.05	.8	27	.082
TNFα	.39	.05	.8	69	.358

AR = Androgen Receptor; VEGF = Vascular endothelial growth factor; TNFa = Tumour necrosis factor alpha.

[a] One-way ANOVA test.

Table S2: The characteristics of the selected antibodies.

Antibody	clonality	Isotype	Host	Reactivity	Tissue specificity	Catalog number	company
Anti-Androgen Receptor clone AR441	Monoclonal	IgG	Mouse	Human	Nucleus	M3562	DAKO
Anti-VEGF clone VG1	Monoclonal	IgG	Mouse	Human	Secreted	M7273	DAKO
Anti-TNFa	Polyclonal	IgG	Rabbit	Mouse, Rat, Guinea pig, Human, Pig, Fish, Cynomolgus monkey	Nucleus and cytoplasm	Ab6671	Abcam

Table S3: The protocol used for AR (1:50), VEGF (1:100) and TNFa (1:200).

Category	Code	Reagent Name	Incubation
Rinse		Buffer	
Enzyme Pre-treatment		FLEX TRIS High PH Solution	10min 97°C
Rinse		Buffer	
Endogenous Enzyme Block	SM801	FLEX Peroxidase Block	5min
Rinse		Buffer	
Primary Antibody		FLEX Ab Diluent + 1° Ab	o/n 4°C
Rinse		Buffer	
Secondary Reagent	SM804	FLEX + Mouse LINKER (LINKER; for VEGF only)	15min
Rinse		Buffer	
Labelled Polymer	SM802	FLEX/HRP	20min
Rinse		Buffer	5min
Substrate-Chromogen	SM803	FLEX DAB + Substrate-Chromogen	5min
Rinse		Buffer	
Auxiliary		Copper-Sulphate 0.5%	5min
Rinse		Buffer	
Counterstain	SM806	FLEX Hematoxylin	5min
Rinse		DI Water	
Rinse		Buffer	5min
Rinse		DI Water	